






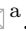





Initial Characterisation of a Prototype TMR Assembly for an Electron-Driven CANS at CERN’s CLEAR Facility

Laurence Wroe ^a, Giorgi Kharashvili ^b, Jonas Okkels Birk ^c, Federico Vanti ^b,
Wilfrid Farabolini ^a, Fares Elattab ^b, Davide Gamba ^a, Torsten Koettig ^a,
Roberto Corsini ^a, Steinar Stapnes ^a, and Francois Plewinski ^b

^aCERN, CH-1211 Geneva-23, Switzerland

^bDAES, CH-1213 Geneva-23, Switzerland

^cDanish Technological Institute, Taastrup, DK - 2630, Denmark

Synopsis

This article presents the design, installation, and first experimental testing of a novel, prototype target–moderator–reflector (TMR) assembly for a compact accelerator-driven neutron source (CANS) driven by a 35 MeV electron beam.

Abstract

The Versatile ULtra-Compact Accelerator-based Neutron source (VULCAN) project is developing a compact accelerator-driven neutron source (CANS) optimised for neutron diffractometry in industrial and university settings. Central to VULCAN is a novel target-moderator-reflector (TMR) assembly optimised to convert a 35 MeV pulsed electron beam into short neutron pulses ($\text{FWHM} \leq 20 \mu\text{s}$) in the 1.5 \AA to 3.5 \AA wavelength range. To validate the simulation-driven design process, a prototype TMR was developed for testing at CERN’s CLEAR facility, and this paper presents the design, installation, and results of the first experimental campaign. While moderated neutron pulses were successfully detected, significant discrepancies were observed between the experimental and simulated energy spectra. Potential causes are discussed and recommendations for follow-up measurements are provided.

Keywords: Neutron scattering; neutron time of flight; CANS; electron linac

1 Introduction

Neutron scattering provides a powerful, non-destructive probe of matter at the atomic scale, offering deep penetration and unique sensitivity to light elements and isotopes (Langel, 2023). It underpins research and innovation across a diverse range of fields from energy and climate to healthcare and advanced manufacturing, “provid[ing] the basis for innovation, new and better products and, in result, societal well-being” (Brückel *et al.*, 2020).

Most neutron scattering instrumentation are hosted at large scale research infrastructures (LSRIs) that use nuclear research reactors or spallation sources to generate neutron net yields of $\gtrsim 1 \times 10^{16}$ n/s and enable the operation of more than 30 instruments in parallel (Findlay *et al.*, 2021). While there are just over 100 LSRIs in operation worldwide (IAEA, 2025a; IAEA, 2025b), the demand for neutrons exceeds supply and many instruments are oversubscribed by more than a factor of two. This imbalance is expected to only worsen as ageing reactors are retired without replacement (Carlile *et al.*, 2016).

Compact accelerator-driven neutron sources (CANS) are a promising route to expand access to neutron techniques beyond LSRIs. They deliver lower energy ($\lesssim 100$ MeV), lower power ($\lesssim 10$ kW) particle beams to target–moderator–reflector (TMR) assemblies optimised to create tailored neutron spectra for specific instrumentation and applications. While providing significantly lower fluxes than their LSRI counterparts, CANS enable scalability through smaller footprint and capital cost, reduced operational complexity and licensing requirements, lower radioactive waste production, and flexibility to tailor instrumentation and sample environments to specific user needs (Brückel *et al.*, 2020).

The Versatile ULtra-Compact Accelerator-based Neutron source (VULCAN) project seeks to realise a turnkey CANS that is optimised for neutron diffractometry in industrial and university settings. Such facilities will utilise a compact electron linear accelerator (linac) to deliver a 35 MeV, kilowatt-scale electron beam to a TMR optimised to generate slow neutrons in the 1.5 Å to 3.5 Å wavelength range for time of flight measurements. A conceptual visualisation is shown in Figure 1, with further details provided in Refs.(Wroe *et al.*, 2026; Wroe *et al.*, 2025).

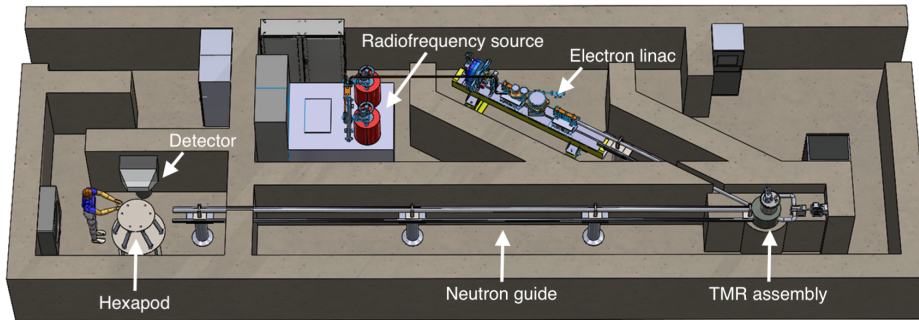


Figure 1: Conceptual visualisation of the VULCAN facility.

Key to the success of VULCAN is a TMR design that efficiently converts the electron beam into the desired slow neutrons. To validate the simulation-based design framework, a prototype TMR was constructed and characterised at CERN’s CLEAR facility. This paper presents the prototype design, experimental setup, and initial results.

The paper is structured as follows: [section 2](#) provides an overview of the experiment, [section 3](#) describes the prototype TMR design, and [section 4](#) details the experimental setup at CLEAR, including installation, modelling, and data processing. [section 5](#) compares the measured neutron yields and spectra with simulation predictions and discusses potential causes for observed discrepancies. [section 6](#) summarises the findings and discusses next steps for future testing.

2 Experimental Overview

The VULCAN concept has been under development since 2021 by an industrial consortium of DAES SA, the Danish Technological Institute, and Xnovo Technology ApS, with support from CERN since 2023. To ensure that the compactness, cost, and complexity of the facility are compatible with its intended performance and business model, VULCAN operates as a time of flight neutron source driven by a pulsed electron linac (Wroe *et al.*, 2026).

Dedicated research and development efforts have focused on the design of a novel, compact TMR assembly capable of converting a pulsed 35 MeV incident electron beam into the desired thermal neutron spectrum. The design targets production of 6 meV to 36 meV neutrons (wavelengths 1.5 Å to 3.5 Å, velocities 1.1 km/s to 2.6 km/s) with an initial pulse full width at half maximum (FWHM) of $\leq 20 \mu\text{s}$ to achieve the needed resolution within a sufficiently compact flight path (order of 10 m) for industrial deployment.

The TMR design has been iteratively developed using the Monte Carlo radiation transport code FLUKA (Ahdida *et al.*, 2022; Battistoni *et al.*, 2015; Donadon, André *et al.*, 2024). To enable early-stage validation of this design process, a prototype TMR assembly based on a decoupled, cold liquid methane moderator and without active target cooling was fabricated to compare measured neutron flux, energy spectrum, and pulse FWHM with simulation predictions. As modelling studies indicated that the temporal pulse structure has significant dependence on neutron poisoning, the prototype was designed to operate in both poisoned and unpoisoned configurations to further validate the modelling framework.

CERN’s CLEAR (CERN Linear Electron Accelerator for Research) facility provided the electron beam for testing the TMR prototype (Gamba *et al.*, 2018). Its 30 m-long beamline includes a spectrometer for energy measurement and a comprehensive suite of diagnostics, including bunch charge monitors, beam position monitors, and YAG screens for beam characterisation. The accelerator optics, as well as the power and phase of the RF fields delivered to each of the four accelerating structures, can be individually and remotely set, enabling a wide range of beam parameters in energy, energy spread, charge, bunch length, and transverse size. CLEAR also provides short access

times to the accelerator hall, with post-operation cooldowns of only 15 min to 30 min permitting multiple adjustments of the experimental setup throughout the day.

Table 1 summarises the electron beam parameters required for the final VULCAN design, those used for optimising the prototype design in simulation, and those attainable at the CLEAR facility. As the prototype TMR lacks active cooling, it was designed to operate at substantially reduced beam power. The main discrepancies between the simulation-optimised conditions and those achievable at CLEAR were the beam energy and transverse beam size at the target. The beam could not be reliably transported below 40 MeV, and its transverse size could not be reduced below 4 mm owing to the relatively large distance between the final set of focusing quadrupoles in CLEAR and the TMR target. To enable direct comparison between simulation and experiment, the beam energy, size, and charge were recorded for each measurement and simulations were subsequently performed using these recorded parameters as inputs.

Table 1: Electron beam parameters required for the final VULCAN design, used for optimising the prototype designs, and achievable at CERN’s CLEAR facility.

Parameter	VULCAN Facility	Prototype Optimisation	CLEAR Attainable
Beam energy	35 MeV	35 MeV	40 MeV
Energy spread	< 1 MeV	< 1 MeV	< 1 MeV
Beam size	0.5 mm	0.5 mm	4 mm
Train length	< 1 μ s	< 1 μ s	< 100 ns
Train charge	\gtrsim 290 nC	–	4 nC
Repetition rate	\sim 100 Hz	–	10 Hz
Beam power	> 1 kW	> 1 W	1.6 W

3 TMR prototype

Figure 2 shows the design of the prototype TMR in the poisoned configuration. Figure 2a presents an external view of the fully assembled structure, Figure 2b shows the interior of the cryostat with the cryostat and borated polyethylene shielding removed, while Figure 2c highlights the borated aluminium decoupler with the outer shielding and lead brick assembly removed. Figure 2d focuses on the methane chamber and its surrounding components, and Figure 2e and Figure 2f illustrate the spatial arrangement of the high-density polyethylene (HDPE) pre-moderator, methane moderator, gadolinium poison, and tungsten tantalum target.

The key, functional components of the TMR annotated in Figure 2 are as follows:

- **Target:** The incident electron beam strikes a cylindrical tungsten tantalum (W10Ta90) target (Figure 2f), 1 cm in radius and 3 cm in length. High-energy (MeV-scale peak) photons are generated via the Bremsstrahlung process

$$e^- + N \rightarrow e^- + N + \gamma,$$

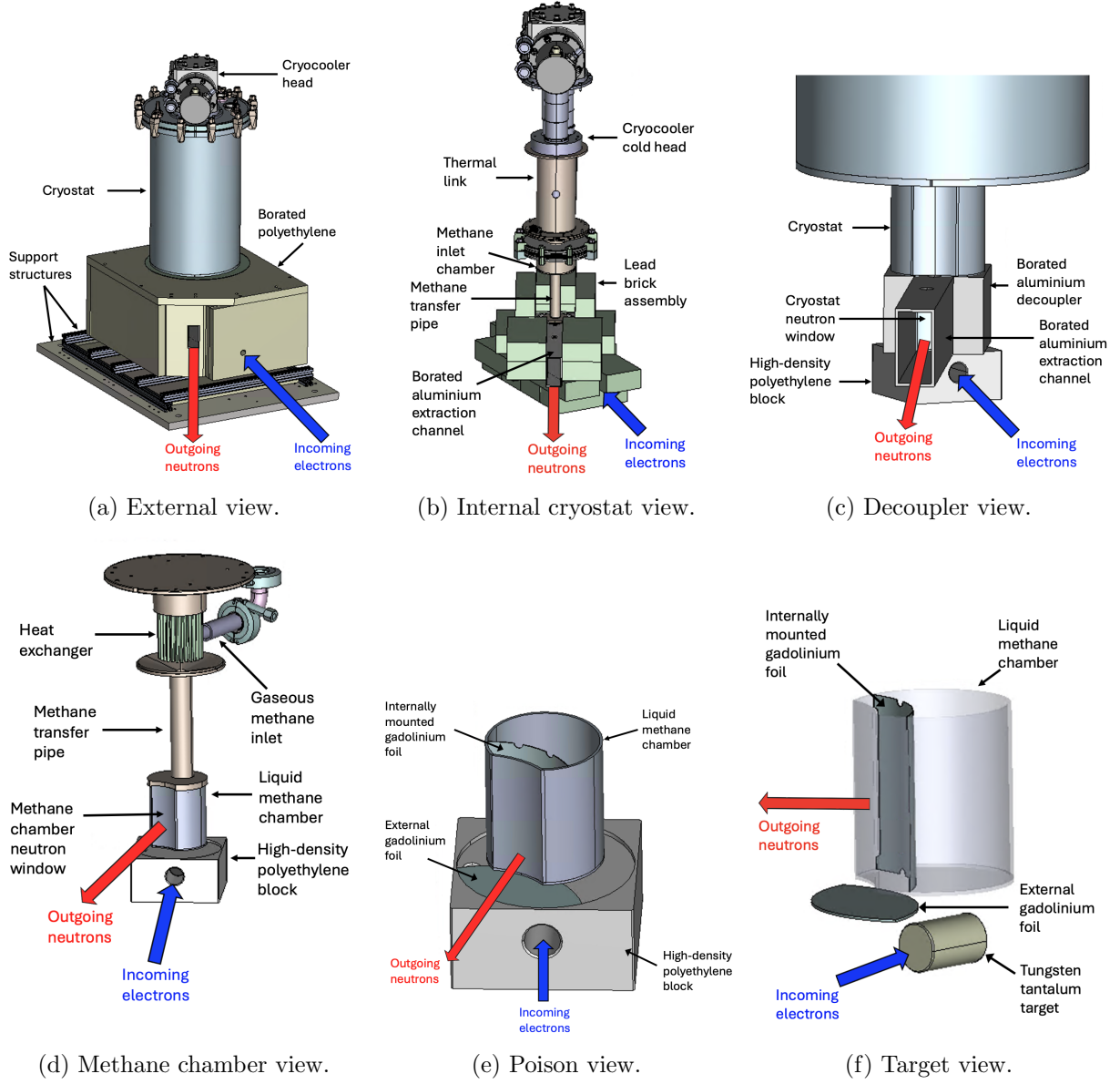


Figure 2: The decoupled-poisoned TMR prototype.

where N represents a nucleus in the target. These photons subsequently produce photoneutrons (MeV-scale peak) through the reaction



where N^* denotes an excited nucleus.

- **Pre-moderator:** The target is encased inside of a $100 \text{ mm} \times 50 \text{ mm} \times 100 \text{ mm}$ high-density polyethylene block (Figure 2c to Figure 2e), which serves the purpose of pre-moderating the photoneutron spectrum before it enters the cold, liquid methane moderator.

- **Moderator:** The methane chamber (Figure 2d to Figure 2f) is positioned inside the TMR cryostat with its bottom face 15 mm above the HDPE pre-moderator. The chamber is cylindrical with a height of 70 mm and a circular cross-section of radius 30 mm, except for the removal of a convex minor segment to create a concave neutron window surface. In operation, the methane chamber holds approximately 85 g (200 mL) of liquid methane at 100 K to moderate neutrons to the meV range. The methane chamber is cooled by a 2-stage cryocooler (Figure 2a and Figure 2b).
- **Poison:** Two different, interchangeable methane chambers were manufactured, allowing the TMR to be configured in either a decoupled-poisoned or decoupled-unpoisoned setup.
 - **Poisoned:** The poisoned configuration includes a 0.05 mm-thick gadolinium foil internally mounted within the methane chamber (Figure 2e and Figure 2f) and an additional external gadolinium foil placed beneath the chamber between the HDPE pre-moderator and the cryostat (Figure 2e and Figure 2f). The internal foil is curved with the same radius of curvature as the neutron window, maintaining a separation of 16 mm between the foil and window surface, optimised for neutron flux and temporal pulse structure¹.
 - **Unpoisoned:** The unpoisoned configuration uses a methane chamber without any internal poison and omits the external gadolinium foil beneath the cryostat.

The effect of neutron poisoning on the temporal pulse structure is illustrated in Figure 3, which shows neutron time spectra at the cryostat neutron window for both configurations. The poisoned configuration approximately reduces both the flux and the initial pulse FWHM of thermal neutrons in the 6 meV to 36 meV range by a factor of two.

- **Decoupler:** A 3 mm-thick borated aluminium (0.31 mass fraction boron carbide, 0.69 mass fraction Al-6061 alloy) shell (Figure 2c) surrounds the cryostat volume housing the methane chamber. The shell is positioned between the cryostat and the lead reflector and provides neutron absorption on all surfaces except the bottom face and the neutron extraction channel, decoupling the moderator from the surrounding reflector.
- **Reflector:** An assembly of lead bricks (Figure 2b) surrounds the HDPE pre-moderator and the methane chamber.
- **Shielding:** The target, pre-moderator, moderator, and reflector components are all enclosed within a 25 mm-thick 5% borated polyethylene box (Figure 2a).
- **Neutron extraction channel:** A 40 mm × 80 mm borated aluminium extraction channel (Figure 2b and Figure 2c) links the concave surface of the cryostat to the outside of the borated polyethylene box. The methane chamber neutron window, cryostat neutron window, and extraction channel are offset from the incoming electron beam direction by 30°.

¹Future TMR designs will also optimise for resolution by, for example, incorporating a flatter moderator surface.

- **Cryostat:** The 316L stainless steel cryostat (Figure 2a and Figure 2b) encloses the cryocooler head and methane chamber, and is evacuated to provide thermal insulation and prevent moisture in the air from freezing on the cryogenic components. The lower section of the cryostat housing the methane chamber is machined with a cryostat neutron window (Figure 2c), a concave surface aligned with the methane chamber neutron window. A gap of 12.5 mm separates the methane chamber window from the cryostat window.
- **Gas line:** A gas line (not shown in Figure 2) is used to flush and evacuate the methane chamber prior to safely filling it with methane. After operation, the gas line is also used to safely evacuate the methane from the TMR.

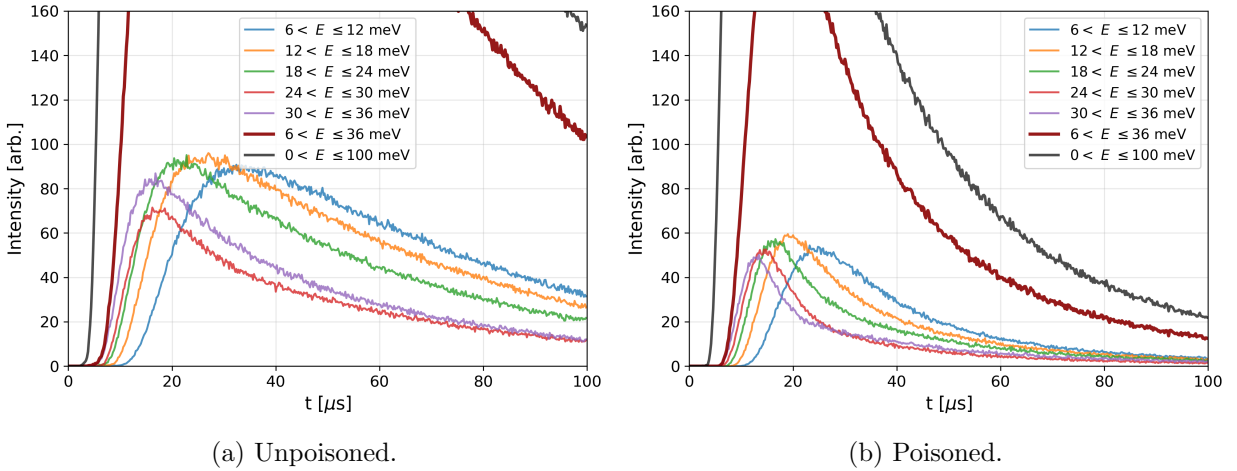


Figure 3: Comparison between the time spectra of slow neutrons at the cryostat neutron window between the unpoisoned and poisoned configurations.

4 Experiment at CLEAR

4.1 Installation

4.1.1 TMR

The cryostat and both poisoned and unpoisoned methane chambers were commissioned in CERN’s Cryolab. Leak testing verified a leak rate below 1×10^{-7} mbar · l/s throughout the system and vacuum tests showed the required vacuum level and stability were attained. The complete operational procedure of gas injection into the methane chamber with a mass flow controller, liquification, storage, and evacuation was also confirmed with argon as a substitute for methane, as the necessary safety measures were not in place for handling methane in the Cryolab. A PID-based temperature control system demonstrated the ability to maintain the methane chamber temperature within ± 2 K.

The TMR was then fully assembled and installed on CLEAR’s in-air test stand, with Figure 4 illustrating the various stages. Following installation, the centre of the TMR target was aligned with

the beam axis using an alignment laser mounted in the CLEAR beamline. A LANEX scintillating screen was affixed to the target face to enable direct measurement of the beam position and size on the target. A ventilation hood and Makrolon curtain were also installed around the test stand to contain any potential methane leakage.

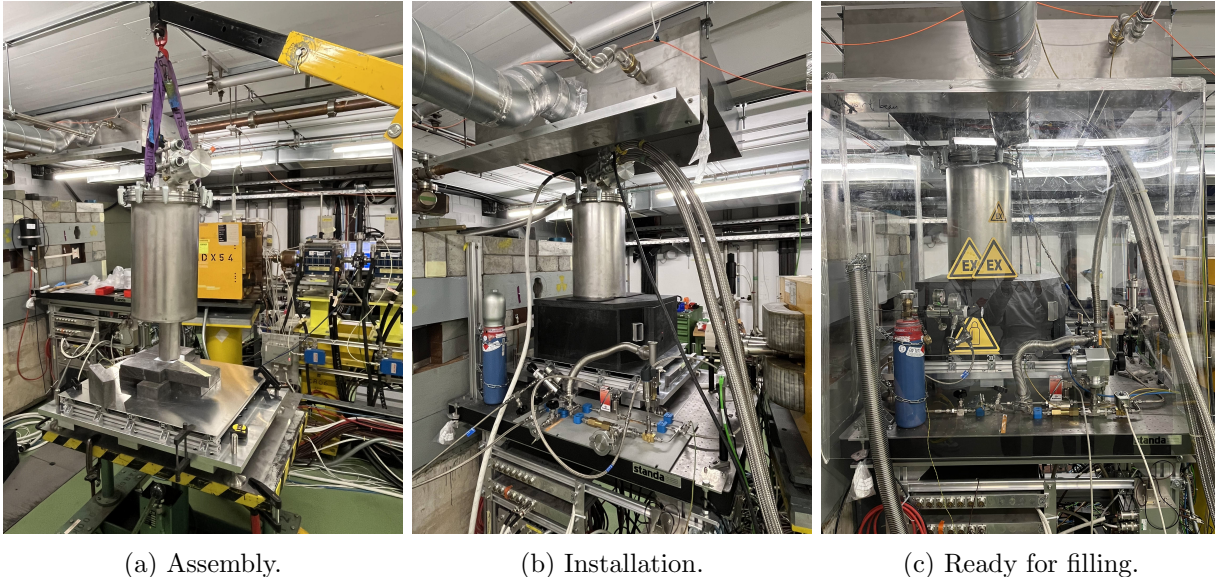


Figure 4: The assembly and installation of the VULCAN TMR in CLEAR.

4.1.2 Detector

A ^3He Monoblock Aluminium Multitube (MAM) detector (Lafont *et al.*, 2022) was used to measure the thermal neutron spectra. The detector, shown in Figure 5a, consists of eight gas-filled proportional counter tubes, with a total active area of $76\text{ mm} \times 96\text{ mm}$. It was installed at distances of 1.6 m, 4.2 m, and 6.6 m from the cryostat neutron window and, to reduce background noise from the prompt γ flash and from radiation originating outside the TMR, the detector was housed within shielding composed of lead and borated polyethylene as shown in Figure 5a. Additional collimation was provided by a tunnel of borated rubber, to further suppress off-axis radiation and improve signal-to-noise in the measured neutron spectrum.

Each tube of the detector was pressurised with 1 bar of ^3He , chosen to optimise the neutron detection efficiency². The detector was operated at a voltage of 1.1 kV to: maximise detection efficiency without over-saturation, allow discrimination between high-energy neutron interactions and lower-energy gamma interactions, and protect the detector from potential overvoltage damage. The detector was configured with $10\text{ }\mu\text{s}$ bin widths and its detection threshold was set above the electronic noise floor. A $5\text{ }\mu\text{s}$ acquisition delay was applied after each beam pulse to suppress the prompt radiation background³.

²The peak measured instantaneous count rate was 60 000 cps per tube. With the detector’s intrinsic dead-time of $< 1\text{ }\mu\text{s}$, the counting saturation loss is $< 6\%$.

³The thermal neutrons arrive well-after the prompt radiation; for example, at the distance of 1.6 m, 25 meV

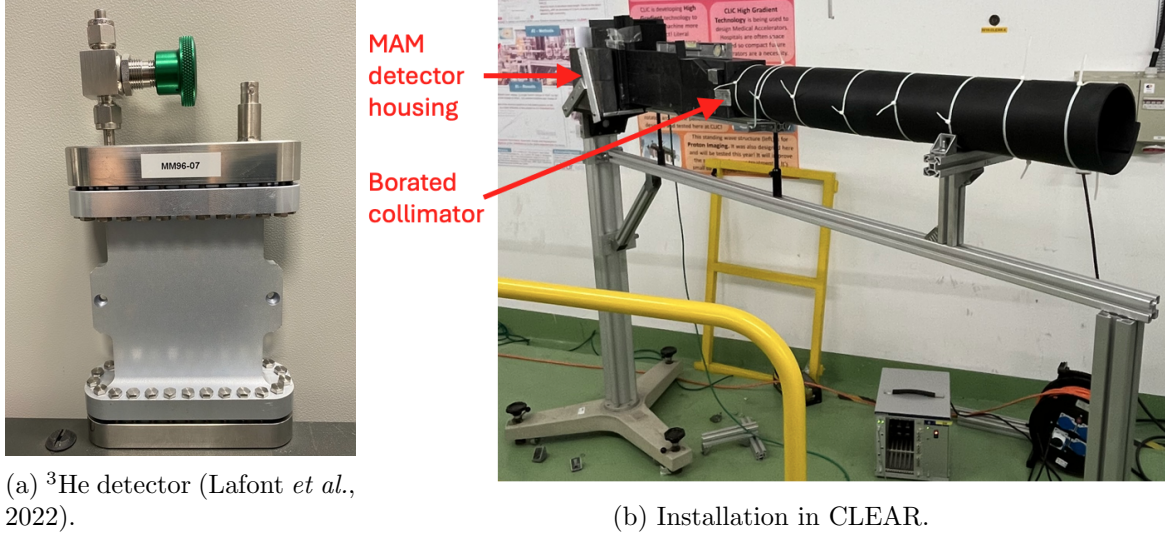


Figure 5: The ^3He detector in the experimental campaign.

4.2 Modelling

The experimental setup in CLEAR was modelled using the FLUKA4-5.0 Monte Carlo code, as shown in Figure 6. Application of appropriate variance reduction techniques allowed modelling of the electron beam interaction with the target, photoneutron production, and neutron moderation processes in a single-step calculation. The pointwise low-energy neutron treatment was activated with the JEFF-3.3 neutron cross-section library applied to all materials. The $S(\alpha, \beta)$ molecular binding correction and Doppler broadening corresponding to liquid methane at 100 K were applied to the moderator material. All other cold materials were modelled at 100 K; except for aluminium and iron which were modelled at 80 K due to the unavailability of $S(\alpha, \beta)$ data at 100 K.

The *USRBDX* card was used to score the average differential flux of neutrons on 73.0 cm^2 surfaces placed at the same locations as the detector in the experiments. The incident electron beam was input with beam parameters recorded for each individual experiment.

4.3 Data Processing

Counts were recorded with the ^3He detector over periods of one hour or longer, with the beam charge and size monitored and adjusted as necessary to maintain the beam specification listed in Table 1. To compare the neutron flux and spectra between the experiments and replicating simulations, data was processed into a differential flux $d\phi/dE$.

4.3.1 Detector Data

The ^3He detector resolved individual counts into one of 256 energy channels and one of 2000 time-channels. The time of flight principle enables conversion of the time channel data into an estimate thermal neutrons arrive at approximately $700\text{ }\mu\text{s}$ after the prompt radiation.

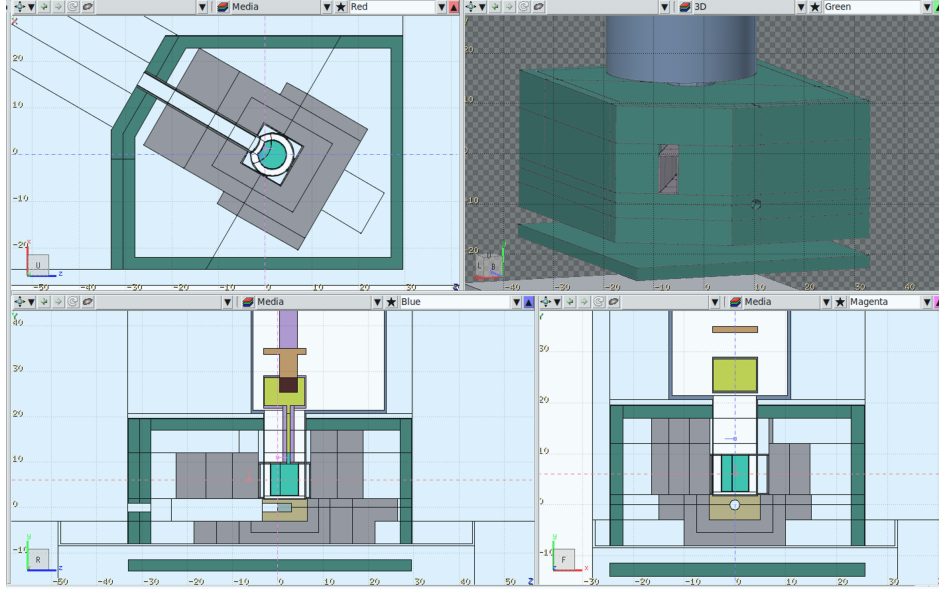


Figure 6: The prototype TMR assembly, as modelled in FLUKA.

of neutron energy distribution as

$$E = \frac{1}{2}m_0 \left(\frac{L}{t} \right)^2, \quad (1)$$

where t is the neutron arrival time, L is the detector-to-source-distance, and $m_0 = 1.675 \times 10^{-27}$ kg is the mass of the neutron⁴.

The differential neutron flux is then calculated as

$$\frac{d\phi}{dE}(E_i) = \frac{N_T(E_i)}{A_{\text{det}}E_{\text{target}}\eta(E_i)\Delta E_i}, \quad (2)$$

where $N_T(E_i)$ is the number of counts in the energy bin centered at E_i with width ΔE_i , $A_{\text{det}} = 73 \text{ cm}^2$ is the active detector area, E_{target} is the total beam energy delivered to the target during a given measurement, and $\eta(E_i)$ is the energy-dependent detection efficiency (for example, 10% at 1.8 Å).

4.3.2 Processing Simulation Data

FLUKA outputs the differential flux $F(E_i)$ in units of $[\text{GeV}^{-1}\text{cm}^{-2}\text{pr}^{-1}]$, where pr denotes the number of primary electrons. The corresponding differential flux, consistent with Equation 2, is therefore

$$d\phi/dE(E_i) = F(E_i)N_e, \quad (3)$$

⁴The initial pulse width can be ignored because the shortest flight path of 1.6 m is sufficiently long (i.e. at 1.6 m, the 700 μs flight time of a 25 meV neutron is much greater than the 20 μs and 60 μs pulse widths of the poisoned and unpoisoned TMRs).

where $N_e = 1.5 \times 10^{14}$ [pr/s/kW] is the number of primary electrons per second per kilowatt for a 40 MeV beam.

5 Spectra Measurements and Comparison with Simulation

5.1 Background

To quantify the background signal in the ^3He detector, a 5 cm-thick borated polyethylene gate was mounted on a movable stage and installed near the aluminium extraction channel exit. The gate could either block the exit or be retracted from it, as shown in [Figure 7a](#).

[Figure 7b](#) compares the thermal neutron spectrum measured at the distance of 1.6 m from the cryostat neutron window with the borated gate inserted, retracted, and the difference between the two. Inserting the gate reduced the measured count rate by approximately 95 %, indicating that the majority of detected events originate from neutrons emitted through the aluminium extraction channel.

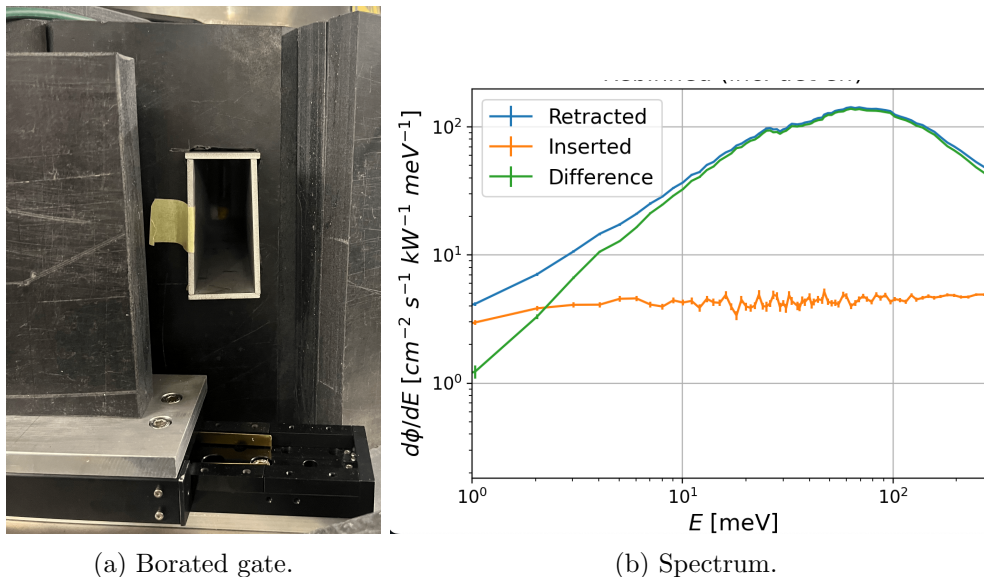


Figure 7: The borated gate shown in the extracted position, leaving the borated aluminium extraction channel exit unobstructed (left). The corresponding measured thermal neutron spectra are shown (right) for: the gate retracted, the gate inserted, and the difference between the two.

5.2 Spectra Comparison

Figure 8 compares the neutron spectra at 1.6 m for: the decoupled-unpoisoned configuration (Figure 8a), decoupled-poisoned configuration (Figure 8b), decoupled-unpoisoned configuration with the methane chamber vented (Figure 8c), and with all datasets on the same plot (Figure 8d).

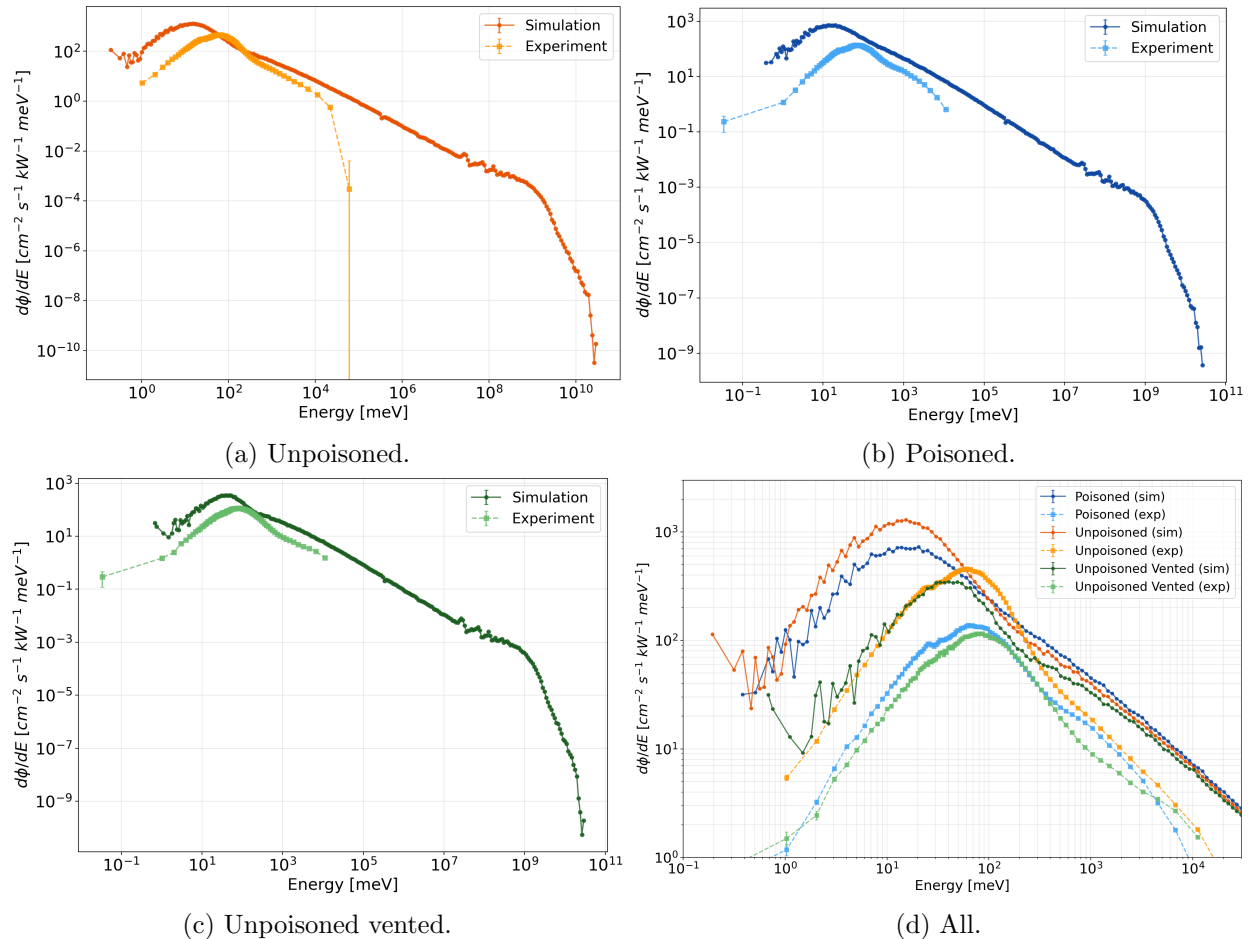


Figure 8: Neutron spectra measured at 1.6 m for the different experimental setups.

The most notable observation is the clear discrepancy in peak energy between experiment (65 meV) and simulation (15 meV) for both unpoisoned (Figure 8a) and poisoned (Figure 8b) configurations. An incorrect moderator temperature could potentially explain this shift, however, the discrepancy persists even when the unpoisoned TMR was warmed to room temperature and vented of methane (Figure 8c), where the peak shifts to 85 meV experimentally compared to 45 meV in simulation⁵. This indicates that the spectral shift cannot be attributed solely to methane moderator conditions, including incorrect fill level, methane loss during operation, or errors in the methane thermal scattering models used in simulations.

Systematic errors in either the detector calibration or simulation setup could also contribute to

⁵Measurements were also taken with the unpoisoned TMR at 92 K, 100 K, and 107 K (temperatures accessible within the experimental setup while maintaining liquid methane) but the change in spectra was too small in both experiment and simulation to provide any significant insight.

the discrepancy. Potential detector-related issues include incorrect time-channel calibration (the reported 10 μ s channel width may not match the actual electronics setting) or misalignment relative to the neutron extraction channel (alignment was performed with lasers but not quantified), while simulation-related errors could include incorrect material property specifications. These potential systematic effects highlight the importance of calibrating the detector against a known neutron source and benchmarking simulations against reference measurements in future experimental campaigns.

Measurements were also taken at 4.1 m and 6.6 m and the flux decay with distance was comparable between simulation and experiment, with spectral shapes were consistent across all three measurement positions. This supports that slow neutrons were being measured with distance linearly proportional to flight time and with initial pulse width negligible to flight time, and that neutron transport beyond the TMR was well-modelled in simulation.

6 Conclusions

This paper has presented the design, installation, and initial characterisation of a novel prototype TMR developed as early-stage validation of the design framework for the Versatile ULtra-Compact Accelerator-based Neutron source (VULCAN) project, which aims to realise a CANS optimised for neutron diffractometry in industrial and university settings. The prototype TMR, with a decoupled liquid methane moderator and configurable in both poisoned and unpoisoned configurations, was tested at CERN's CLEAR facility using a 40 MeV, 1.6 W electron beam to benchmark simulation predictions of thermal neutron production, transport, and temporal characteristics against experimental measurements.

Neutron spectra recorded using a ^3He detector demonstrated the detection of thermal neutrons, with approximately 95% of recorded counts originating from the neutron extraction channel of the TMR. However, significant discrepancies were observed in the measured energy spectra, with a 65 meV peak energy experimentally measured for the poisoned and unpoisoned TMRs filled with liquid methane compared to an expected 15 meV peak from simulation. This difference in peak energy persisted even when the TMR was warmed to room temperature and vented of methane (85 meV vs 45 meV), indicating the cause extends beyond issues with the moderator operation or thermal scattering model accuracy. Other potential contributors include systematic errors in detector time-channel calibration, detector positioning uncertainties relative to the extraction channel, or simulation setup.

Despite these discrepancies, the measurements establish a foundation for future work. The prototype TMR was successfully fabricated, commissioned, and operated in both configurations, validating the practical aspects of construction, installation, and operation that are also essential to project VULCAN. The installation procedure at CLEAR was derisked, and the facility was demonstrated as suitable for pulsed neutron characterisation experiments.

Recommended next steps include calibrating the ^3He detector in-situ against a known neutron source to eliminate systematic uncertainties in detector setup. Simulation models can also be benchmarked using the same reference source to check data processing techniques. Additionally, methods to directly monitor the temperature and fill volume of the moderator during operation should be sought, and the effect of detector misalignment with respect to the neutron extraction channel quantified. Future experimental campaigns should incorporate a crystal diffractometer or a chopper-based system to accurately measure the initial FWHM of the generated neutron pulse at specific wavelengths and compare the results between the poisoned and unpoisoned configurations. Additional TMR prototypes incorporating active cooling would enable operation at beam powers closer to the final VULCAN specification ($>1\text{ kW}$), while exploration of alternative moderator materials may offer improved performance. Resources are currently being sought to fund these next steps and further advance the VULCAN project.

Acknowledgements

The authors wish to thank Bruno Guerard, Julien Marchal, Paolo Mutti, and Franck Rey of Institut Laue-Langevin for lending the neutron detectors and assisting with the operation, installation, and data interpretation. The authors are also grateful to the CLEAR operations team for their support and assistance during the measurement campaign.

Funding

We acknowledge funding by the CERN Knowledge Transfer Fund, the CERN Innovation Programme on Environmental Applications (CIPEA), and the EUREKA-EUROSTARS grant (EUROSTARS E! 115722 - VULCAN).

Conflicts of interest: None.

Data availability: The experimental data and code is available from the authors upon reasonable request.

References

- Ahdida, C., Bozzato, D., Calzolari, D., Cerutti, F., Charitonidis, N., Cimmino, A., Coronetti, A., D'Alessandro, G. L., Donadon Servallo, A., Esposito, L. S., Froeschl, R., García Alía, R., Gerbershagen, A., Gilardoni, S., Horváth, D., Hugo, G., Infantino, A., Kouskoura, V., Lechner, A., Lefebvre, B., Lerner, G., Magistris, M., Manousos, A., Moryc, G., Ogallar Ruiz, F., Pozzi, F., Prelipcean, D., Roesler, S., Rossi, R., Sabaté Gilarte, M., Salvat Pujol, F., Schoofs, P., Stránský, V., Theis, C., Tsinganis, A., Versaci, R., Vlachoudis, V., Waets, A. & Widorski, M. (2022). *Front. Phys.* **9**, 788253.
<https://cds.cern.ch/record/2806210>
- Battistoni, G., Boehlen, T., Cerutti, F., Chin, P. W., Esposito, L. S., Fassò, A., Ferrari, A., Lechner, A., Empl, A., Mairani, A., Mereghetti, A., Ortega, P. G., Ranft, J., Roesler, S., Sala, P. R., Vlachoudis, V. & Smirnov, G. (2015). *Annals of Nuclear Energy*, **82**, 10–18. Joint International Conference on Supercomputing in Nuclear Applications and Monte Carlo 2013, SNA + MC 2013. Pluri- and Trans-disciplinarity, Towards New Modeling and Numerical Simulation Paradigms.
<https://www.sciencedirect.com/science/article/pii/S0306454914005878>

- Brückel, T., Eliot, E., Gutberlet, T., Menelle, A. & Ott, F. (2020). *Low Energy Accelerator-driven Neutron Sources*. Tech. rep. LENS Ad-hoc Working Group.
- Carlile, C., Petrillo, C., Carpineti, M. & Donzelli, M. (2016). *Neutron scattering facilities in Europe Present status and future perspectives*. Tech. rep. ESFRI Physical Sciences and Engineering Strategy Working Group.
- Donadon, André, Hugo, Gabrielle, Theis, Christian & Vlachoudis, Vasilis (2024). *EPJ Web Conf.* **302**, 11005.
<https://doi.org/10.1051/epjconf/202430211005>
- Findlay, D., Thomason, J., Fletcher, S., de Laune, R. & Cooper, E. (2021). *A Practical Guide to the ISIS Neutron and Muon Source*. Science Technology and Facilities Council.
- Gamba, D., Corsini, R., Curt, S., Doebert, S., Farabolini, W., Mcmonagle, G., Skowronski, P., Tecker, F., Zeeshan, S., Adli, E., Lindstrøm, C., Ross, A. & Wroe, L. (2018). *Nuclear Instruments and Methods in Physics Research Section A: Accelerators, Spectrometers, Detectors and Associated Equipment*, **909**, 480–483. 3rd European Advanced Accelerator Concepts workshop (EAAC2017).
<https://www.sciencedirect.com/science/article/pii/S0168900217313311>
- IAEA (2025a). Accelerator knowledge portal.
<https://www.iaea.org/resources/databases/accelerator-knowledge-portal>
- IAEA (2025b). Research reactor database.
<https://www.iaea.org/resources/databases/research-reactor-database-rrdb>
- Lafont, F., Barkats, D., Buffet, J.-C., Cuccaro, S., Guerard, B., Lai, C.-C., Marchal, J., Pentenero, J., Sartor, N., Hall-Wilton, R., Kanaki, K., Robinson, L. & Svensson, P.-O. (2022). *Journal of Instrumentation*, **17**(05), P05043.
<https://dx.doi.org/10.1088/1748-0221/17/05/P05043>
- Langel, W. (2023). *ChemTexts*, **9**(1), 12.
<https://doi.org/10.1007/s40828-023-00184-7>
- Wroe, Wuensch, Walter, Latina, Andrea, Herrador, Javier Olivares & Stapnes, Steinar (2025). *Eur. Phys. J. Spec. Top.* pp. 1–7.
<https://doi.org/10.1140/epjs/s11734-025-01827-1>
- Wroe, L. M., Olivares-Herrador, J., Wuensch, W., Latina, A. & Stapnes, S. (2026). Next-generation electron linear accelerators for compact accelerator-driven neutron sources. Forthcoming.